JACS
JOURNAL OF THE AMERICAN CHEMICAL SOCIETY

ARTICLE

pubs.acs.org/JACS

Plasticity of the Nickel(II) Coordination Environment in Complexes with Hemilabile Phosphino Thioether Ligands

Charles W. Machan, Alexander M. Spokoyny, Matthew R. Jones, Amy A. Sarjeant, Charlotte L. Stern, and Chad A. Mirkin*

Department of Chemistry and the International Institute for Nanotechnology, Northwestern University, 2145 Sheridan Road, Evanston, Illinois 60208, United States

Supporting Information

ABSTRACT: A series of homoligated Ni(II) complexes formed from two phosphino thioether (P,S) chelating ligands has been synthesized and characterized. Interestingly, this included octahedral Ni(II) complexes which, unlike previously characterized d^8 Rh(I), Pt(II), and Pd(II) analogues, exhibit in situ exchange processes centered around chloride ligand dissociation. This was verified and studied through the controlled abstraction from and introduction of chloride ions to this system, which showed that these processes proceed through complexes with square pyramidal, tetrahedral, and square planar geometries. These complexes were studied with a variety of characterization methods, including single-crystal X-ray diffraction studies, solution $^{31}P\{^1H\}$ NMR spectroscopy, UV−vis spectroscopy, and DFT calculations. A general set of synthetic procedures that involve the use of coordinating and noncoordinating counteranions, as well as different hemilabile ligands, to mediate geometry transformations are presented.

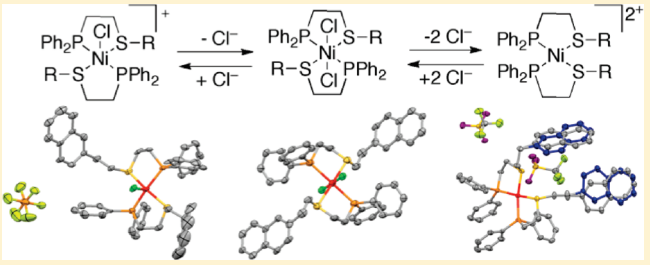

INTRODUCTION

Several coordination-chemistry-based methods for preparing supramolecular macrocycles, tweezers, and cage structures have been developed.[1−11] One of these is the weak-link approach (WLA),[12] which can be used to synthesize inorganic complexes of various and complex geometries from readily available hemilabile ligands **1** and metal precursors (Scheme 1).[13−20] Importantly, the species formed from the WLA can be interconverted between rigid and flexible structures (**2** and **3**, respectively) through small-molecule reactions at the metal sites, thus providing a powerful platform for constructing abiotic allosteric enzyme mimics.[21−23] The approach is extremely general and has been applied to many different metal centers,[24−27] which has substantially increased the scope of its utility in catalysis and biomimetic systems. The ability to form closed complexes with a variety of metal centers (mostly d^8) and appropriate hemilabile ligands has created a library of chemical reactions that involve the use of small molecules or elemental anions to control the in situ closing and opening of such complexes, often into catalytically active forms.[28−30]

Interestingly, Ni(II) is conspicuously absent from the list of metal centers that has been explored with respect to the WLA. Since Ni(II) is known to have a wide range of stable geometries,[31−39] we decided to investigate the potential of using it to form homoligated structures from phosphinoethyl thioether (P,S) hemilabile ligands.[40−44] In this paper, we focus on model ligands to map out the possible reactions that could be extended to larger and more complex ligands capable of forming tweezers and macrocycles, similar to the ones studied in the context of other transition metal centers.[13−18,20,24]

Scheme 1. Scheme for the Formation and Reversible Allosteric Control of the Conformations of Supramolecular Macrocycles Using the WLA

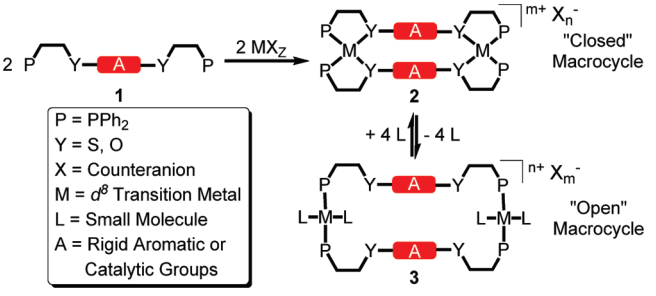

Herein, we report the discovery of new P,S Ni(II) bis-chelate complexes, which have coordination modes that can be reversibly switched between octahedral, square pyramidal, tetrahedral, and square planar geometries via the controlled introduction and subsequent abstraction of equivalents of halide ion(s), respectively (Scheme 2). Analogous reactions have been explored with

Received: October 26, 2010
Published: February 14, 2011

dx.doi.org/10.1021/ja109624m | J. Am. Chem. Soc. 2011, 133, 3023–3033

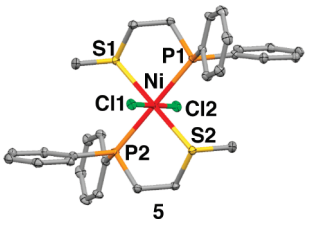

Figure 1. Single-crystal X-ray crystallographically derived structure of **5**. Thermal ellipsoids are drawn at 50% probability. Hydrogen atoms have been omitted for clarity; P = orange, S = yellow, Ni = red, C = gray, and Cl = green.

Scheme 2. Reaction Scheme for Formation of 5, 8a−d, 9a,b, d, and 10a−c[a]

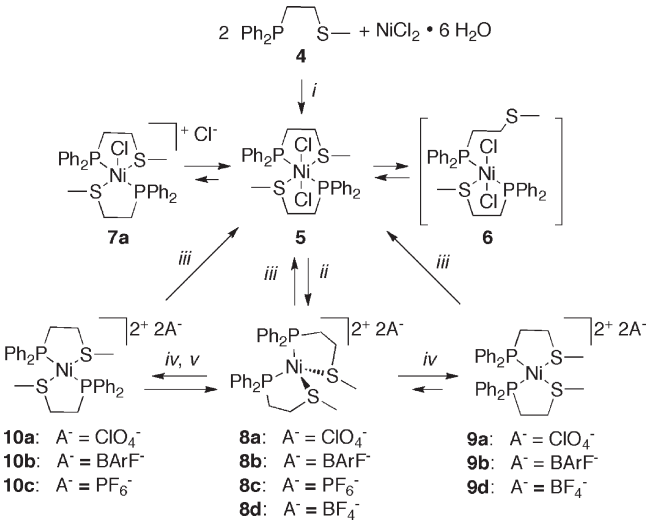

[a] (i) EtOH, 1 h; (ii) **8a**, 2 equiv of $LiClO_4$ in $EtOH/CH_2Cl_2$, 1 h; **8b**, 2 equiv of NaBArF in CH_2Cl_2, 1 h; **8c**, 2 equiv of $TlPF_6$ in CH_2Cl_2, 1 h; **8d**, 2 equiv of $AgBF_4$ in CH_2Cl_2; (iii) 2 equiv of bis(triphenylphosphine)iminium chloride (PPN^+Cl^-) in CH_2Cl_2; (iv) single crystals of **9a**, **9d**, **10b**, **10c** grown from CH_2Cl_2 solutions of **8a**, **8b**, **8c**, and **8d** layered with Et_2O; (v) **10a**, excess $LiClO_4$ in CH_2Cl_2, 3 days, single crystals were grown by layering the reaction solution with Et_2O.

several P,S ligand systems, where the coordination geometry of the complexes can be modulated by the deliberate and controlled introduction of halide ion (vide infra). Given the generality of these reactions with respect to Ni(II), this system provides a basis for constructing new Ni(II)-based allosterically regulated catalysts and abiotic enzyme mimics, with chemical reactivities that complement the other d^8 systems studied to date.[1,20,21,25−28,30]

RESULTS AND DISCUSSION

Synthesis of Complex 5. To evaluate the reactivity of Ni(II) in the context of the WLA and known P,S ligands, we reacted nickel(II) chloride hexahydrate ($NiCl_2 \cdot 6H_2O$) in ethanol at room temperature with 2 equiv of ligand **4**[25] (Scheme 2). After 1 h, complex **5**, *trans*-$[\kappa_2\text{-}(Ph)_2PCH_2CH_2SCH_3]_2Ni(Cl)_2$, formed in near quantitative yield as evidenced by $^{31}P\{^1H\}$ NMR spectroscopy and a color change from pale green to deep red. The $^{31}P\{^1H\}$ NMR spectrum of **5** in CD_2Cl_2 revealed a broad singlet at δ 32, which is approximately 50 ppm downfield with respect to free ligand **4**, consistent with ligand coordination. All other

Table 1. Selected Bond Length and Bond Angle Data for the Crystallographically Derived Structures of 5, 9a, and 10a

bond lengths (Å)	5	9a	10a
P1−Ni	2.4719(3)	2.1848(12)	2.2172(4)
P2−Ni	2.4719(3)	2.1832(12)	2.2172(4)
S1−Ni	2.4520(3)	2.2207(12)	2.1830(4)
S2−Ni	2.4520(3)	2.2149(12)	2.1830(4)
Cl1−Ni	2.3674(2)	n/a	n/a
Cl2−Ni	2.3674(2)	n/a	n/a
bond angles (deg)	**5**	**9a**	**10a**
P1−Ni−P2	180.000(6)	98.90(5)	180.0
P1−Ni−S1	84.643(6)	86.72(4)	87.204(14)
P1−Ni−S2	95.357(6)	172.78(5)	92.795(14)
P2−Ni−S1	95.357(6)	174.39(5)	92.795(14)
P2−Ni−S2	84.643(6)	87.60(4)	87.205(14)
S1−Ni−S2	180.000(7)	86.80(4)	180.0

spectroscopic and elemental analysis data are consistent with the proposed solution structure for **5**. Single crystals of **5**, suitable for X-ray diffraction analysis, were grown by layering diethyl ether (Et_2O) on top of **5** dissolved in CH_2Cl_2 in an NMR tube (Figure 1). The solid-state structure of **5** consists of a Ni center chelated by 2 equiv of ligand **4**. The phosphine and thioether moieties are in a trans arrangement, with two chloride atoms coordinated to the open axial positions of the metal, giving rise to an octahedral geometry. Although there are no crystallographically characterized octahedral Ni complexes with bidentate phosphinoalkyl thioether hemilabile ligands, the P−Ni and S−Ni bond lengths are consistent with analogous bond lengths in previously reported structures with monodentate phosphines and thioether ligands.[40,42,45−48] Whether **5** should be referred to as a 20-electron complex is debatable,[49] but regardless, the lability of both the Ni−Cl and Ni−S interactions is unambiguous in solution, which indicates that the solid-state structure is not representative of the species in solution. The Ni−Cl bonds in **5** are relatively unchanged from the reported Ni−Cl length of 2.38 Å for nickel(II) chloride hexahydrate[50] [2.3674(2) Å]. The P1−Ni−S1 and P2−Ni−S1 angles in the equatorial plane around the Ni(II) center deviate from 90° by approximately 5° (Table 1), likely a consequence of the bite angle of chelating ligand **4**.[51]

In order to determine the reason for the observed broadening in the $^{31}P\{^1H\}$ NMR spectrum of **5**, we conducted a variable temperature (room temperature to 213 K) NMR study of this complex in CD_2Cl_2. As the sample temperature is decreased, the initially broad resonance at δ 32 resolves into two resonances at 253 K with a major peak at δ 57 and a minor one at δ 30. This process is completely reversible (Figure 2). One possible explanation for the appearance of two resonances at low temperature in the $^{31}P\{^1H\}$ NMR spectrum of **5** relates to the lability of the Cl^- ligands and their exchange from inner to outer sphere on a time scale too fast to be observed by $^{31}P\{^1H\}$ NMR spectroscopy at room temperature. This result is similar to that observed for an analogous mononuclear Rh(I) tweezer complex.[52] When **5** is dissolved in a more polar solvent (such as ethanol), the $^{31}P\{^1H\}$ NMR spectrum shows three broad resonances at δ 54, 32, and −14 (Figure SI-1, Supporting Information) instead of the single broad resonance observed in CD_2Cl_2. The resonance at δ −14 is downfield from the one observed for the free ligand in ethanol (δ −16) and is thought to arise from a complex with

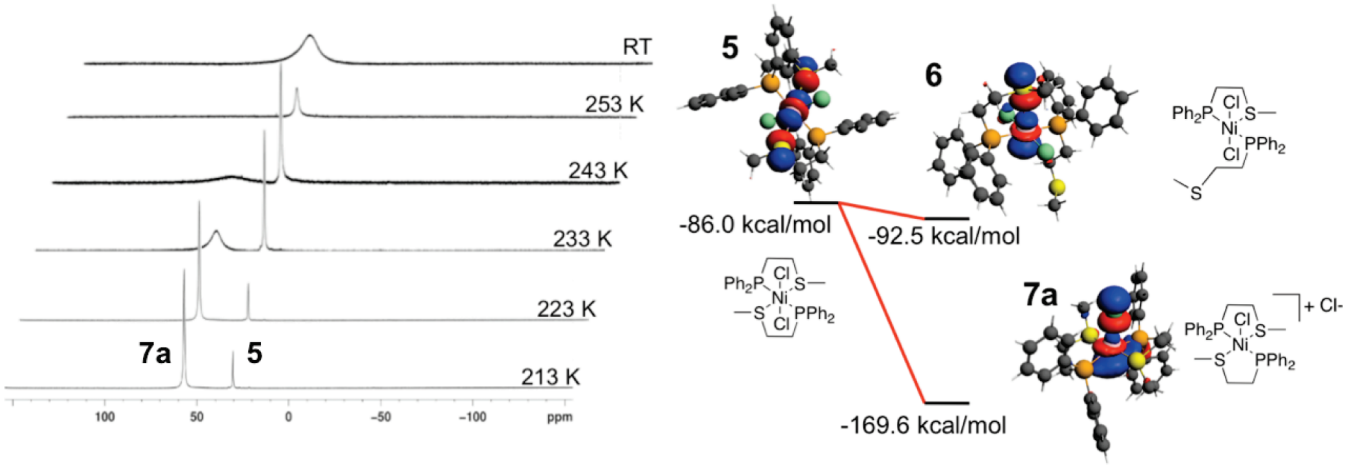

Figure 2. $^{31}P\{^{1}H\}$ VT-NMR spectra of **5** in CD_2Cl_2 and HOMO level comparison of **5**, **6**, and **7a** based on DFT calculations using ADF 2009.01 software. Kohn−Sham representations of frontier orbitals were generated by the ADF 2009.01 GUI.

Scheme 3. Reaction Scheme for Formation of 7a′ [a]

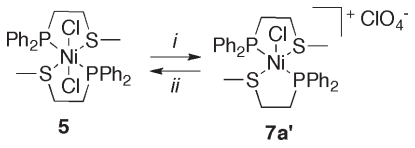

[a] (i) 1 equiv of $LiClO_4$ in $EtOH/CH_2Cl_2$, 1 h; (ii) 1 equiv of PPN^+Cl^- in CH_2Cl_2.

a monodentate version of ligand **4** formed via exchange with ethanol at the metal-bound phosphine site based on literature precedent for this type of reaction.[53] The other two resonances are assigned to **5** and **7a**, respectively (Figure 2). The assignment of these resonances will be corroborated further in the section below describing DFT calculations.

When **5** is dissolved in a less polar solvent such as chlorocyclohexane, a single well-resolved resonance is observed at δ 27. Since less polar solvents stabilize charged intermediates less effectively than polar solvents,[52,54] rapid room-temperature exchange between **5**, **6**, and **7a** is prevented. In addition, we synthesized compound **7a′**, an analogue of **7a**, by the abstraction of a Cl^- ligand from **5** with 1 equiv of lithium perchlorate ($LiClO_4$, Scheme 3) (**SAFETY NOTE**: metal perchlorate salts are potentially explosive and should only be handled with care). Significantly, complex **7a′**, when dissolved in CD_2Cl_2, exhibits a low-temperature $^{31}P\{^{1}H\}$ NMR resonance almost identical to the one assigned to **7a** in CD_2Cl_2 (at 213 K δ 57 for **7a′**, δ 57 for **7a**). At room temperature, compound **7a′** exhibits a broad resonance at δ 52 in its $^{31}P\{^{1}H\}$ NMR spectrum, which is not observed for **5**. This observation may be due to an exchange between five-coordinate species in the presence of only a single chloride ligand in **7a′**, but this has not been fully characterized. In **7a**, the extra Cl^- ligand can participate in a series of exchange reactions involving the displacement of either the phosphine, Cl^-, or thioether at the metal center, causing further signal broadening.[53] Although we were unable to grow single crystals of **7a**, all other characterization data are consistent with its proposed formulation. In addition, an analogous complex **13**, which will be discussed later, has been synthesized and characterized in solution and the solid-state. Its NMR data are almost identical to that for **7a′**.

DFT Calculations on Complex 5. In order to more fully understand **5** and its relation to the possible intermediates observed by $^{31}P\{^{1}H\}$ NMR spectroscopy (and the identity of these intermediates), we have explored the electronic structures of **5**, **6**, and **7a** and some possible intermediates (**7b**−**d**, Figures 3 and 4) with DFT calculations (see Experimental Section). Interestingly, the primary difference between the HOMO and HOMO−1 levels of **5** is the location of the antibonding orbitals between Ni and the coordinating S and Cl moieties (compare Figure 3B with 3C). In the case of the HOMO level, the occupied antibonding orbitals are located on the Ni and S atoms, whereas in the HOMO−1 level, the occupied antibonding orbitals are located on the Ni and Cl atoms. The LUMO level is composed of orbitals involved in antibonding interactions between Ni, P, and Cl. Since a five-coordinate complex is a likely intermediate in the observed $^{31}P\{^{1}H\}$ NMR exchange processes, we calculated the energies of several such complexes (**6**, **7a**−**d**). The energy calculated for the HOMO level of a five-coordinate complex where a single Cl^- has been removed (**7a**) is approximately 77 kcal/mol lower than the analogous level for a five-coordinate complex where a Ni−S bond has been broken (**6**, Figure 2). Upon the basis of pure thermodynamic arguments (inherent intermediate complex stability), the DFT results suggest an exchange centered around Cl^- ligand dissociation, as opposed to the breaking of P−Ni or S−Ni bonds.

Taking the $^{31}P\{^{1}H\}$ VT-NMR spectroscopic data and DFT calculations collectively into consideration allows us to propose a set of reasonable exchange processes involving **5**, **6**, and **7a**−**d** (Figure 4). Upon cooling a solution of **5** in CD_2Cl_2, one begins to observe different isomeric structures as a result of slower exchange at lower temperatures. The upfield resonance at δ 30, which appears at 253 K (Figure 2), is assigned to a static structure (**5**), based on the similarity to the sharp $^{31}P\{^{1}H\}$ NMR resonance of **5** observed in chlorocyclohexane (δ 27) at room temperature. If **6** exists under these conditions, it is in rapid exchange with the other isomers, since one would expect multiple $^{31}P\{^{1}H\}$ NMR resonances for the magnetically inequivalent P atoms in this complex. At temperatures below 253 K, in addition to the resonance at δ 30, a single downfield resonance is observed at δ 57, which has been assigned to **7a** upon the basis of its similarity to **7a′** (δ 57). The DFT calculations suggest that isomers **7b**−**d** are also possible intermediates, but if these exist, they are in rapid exchange with **7a** at low temperature. However, both of the resonances for **5** and **7a** are clearly resolved at 213 K,

dx.doi.org/10.1021/ja109624m | J. Am. Chem. Soc. 2011, 133, 3023–3033

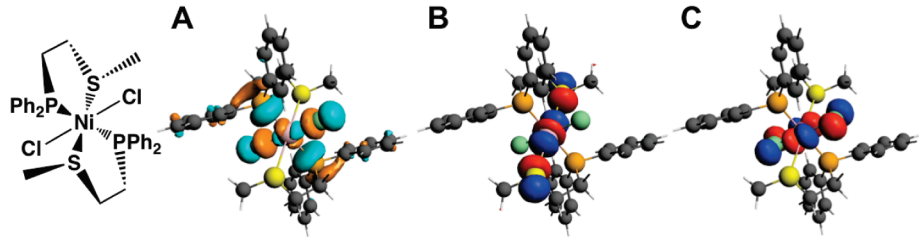

Figure 3. Kohn−Sham representations of the HOMO−LUMO orbitals of **5** were generated from DFT calculations made using the ADF 2009.01 software suite (See Computational Details, Supporting Information): (A) LUMO, −67.3 kcal/mol; (B) HOMO, −86.0 kcal/mol; (C) HOMO−1, −94.9 kcal/mol.

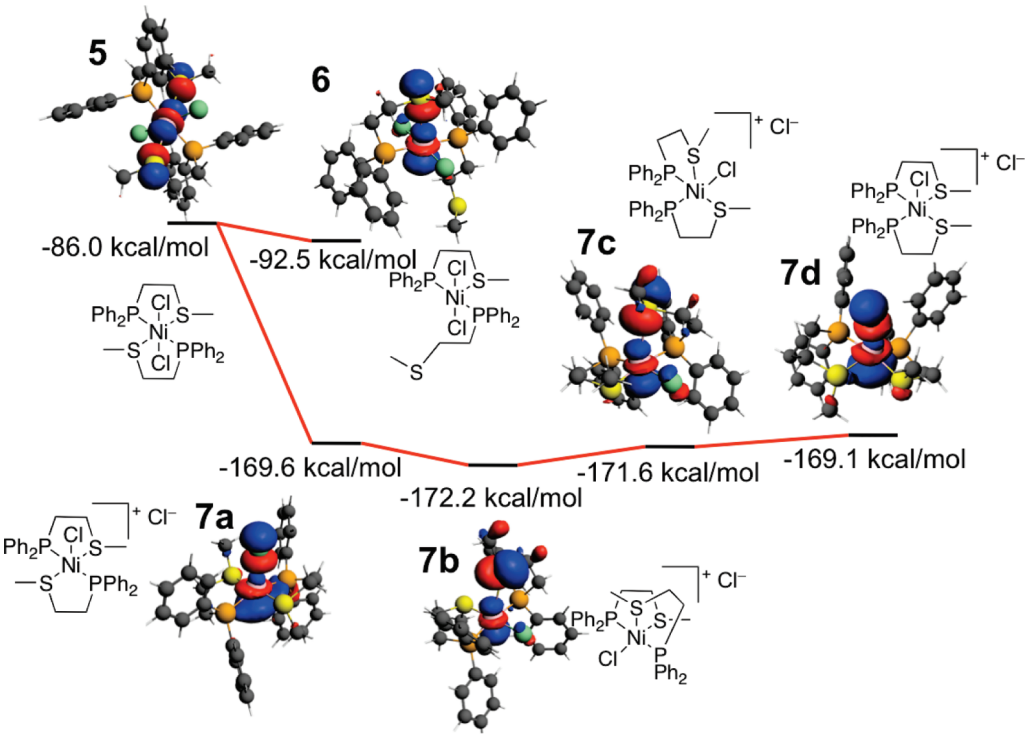

Figure 4. Kohn−Sham representations of HOMO energy levels in the geometry-optimized structures of **5**, **6**, and **7a**−**d** were obtained with DFT calculations using the ADF 2009.01 software suite.

the lowest temperature probed. The broad resonance for **5** at δ 30 is not observed until the sample is warmed to room temperature. Note that the DFT calculations serve as a qualitative way to explain these processes and do not attempt to quantitatively assess the complexity of the exchange processes for **5**, **6**, and **7a**−**d**. Therefore, we hypothesize that this downfield resonance at δ 57 can be assigned to **7a** instead of **7b** (the lowest energy species) since for **7b** one would expect two unique resonances in the $^{31}P\{^{1}H\}$ NMR spectra, due to its magnetically inequivalent phosphorus moieties. We cannot dismiss the possibility that this resonance at δ 57 represents an averaged signal of two or more penta-coordinate isomers derived from **5** (**7a**−**d**) exchanging rapidly even at 213 K.

Synthesis and Characterization of Complexes 8a, 9a, and 10a by the Abstraction of Cl^- Ligands from 5. Since both theoretical and experimental data suggest a potentially labile Ni−Cl interaction, we decided to study the chemical abstraction of Cl^- from **5** to better understand the aforementioned exchange processes and reactivity of **5**. Two equivalents of lithium perchlorate ($LiClO_4$), dissolved in ethanol, were added to a solution of complex **5** dissolved in CH_2Cl_2 at room temperature

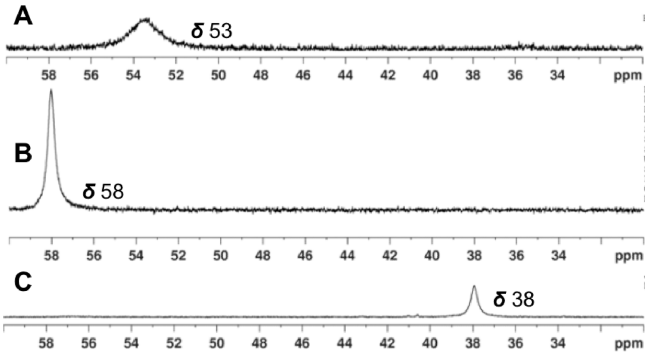

Figure 5. $^{31}P\{^{1}H\}$ NMR spectra of **8a** (A), **9a** (B), and **10a** (C).

(see **SAFETY NOTE**). The reaction mixture was vigorously stirred for 1 h prior to solvent removal under vacuum. The resulting red-orange powder was dissolved in CH_2Cl_2 to form a red mixture, which was filtered to remove LiCl and then taken to dryness in vacuo, leaving a red-orange powder, **8a**. The $^{31}P\{^{1}H\}$

dx.doi.org/10.1021/ja109624m |*J. Am. Chem. Soc.* 2011, 133, 3023–3033

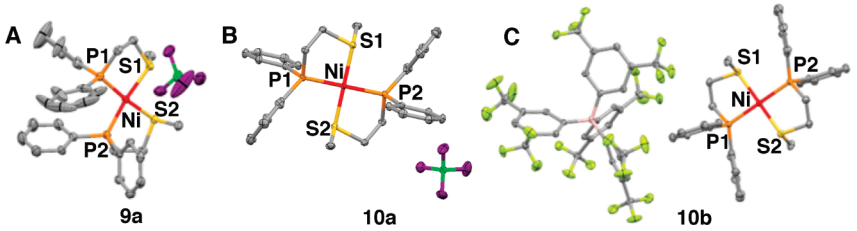

Figure 6. Single-crystal X-ray crystallographically derived structures of **9a** (A), **10a** (B), and **10b** (C) with thermal ellipsoids drawn at 50% probability. Hydrogen atoms and some counteranions are omitted for clarity; P = orange, S = yellow, Ni = red, C = gray, Cl = green, O = purple, F = light green, and B = light pink.

Scheme 4. Reaction Scheme for Formation of 8a, 9a, and 10a ($A^- = ClO_4^-$)[a]

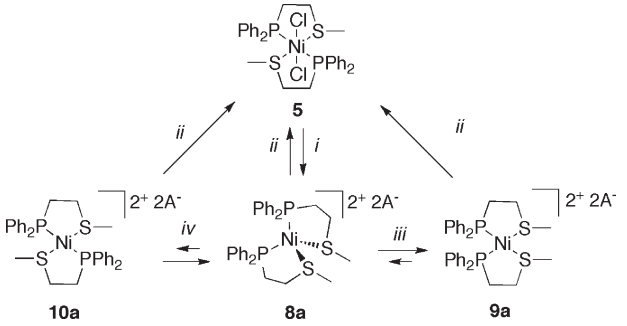

[a] (i) 2 equiv of $LiClO_4$ in $EtOH/CH_2Cl_2$, 1 h; (ii) 2 equiv of PPN^+Cl^- in CH_2Cl_2; (iii) solvent layering a CH_2Cl_2 solution of **8a** with Et_2O; (iv) **10a**: excess of $LiClO_4$ in CH_2Cl_2, 3 days; single crystals were grown by layering the reaction solution with Et_2O. The arrow lengths between **8a**, **9a**, and **10a** represent the relative stability of each species with regard to the others.

NMR spectrum of **8a** dissolved in CD_2Cl_2 exhibits a single broad resonance at δ 53 (Figure 5A). Interestingly, when we attempted to grow crystals of **8a** by layering Et_2O on top of a CD_2Cl_2 solution of **8a**, we obtained crystals of a new pale yellow compound, **9a** (Scheme 4). A single-crystal X-ray diffraction study of **9a** shows that its Ni center is free of Cl^- ligands and has a nearly square planar geometry. To our surprise, ligands **4** in **9a** are in a cis configuration, unlike the trans configuration observed in octahedral **5**. As expected, when the yellow crystals of **9a** were dissolved in CD_2Cl_2, the color and the observed $^{31}P\{^1H\}$ NMR spectrum did not match those for the CH_2Cl_2 solution of **8a**. The solution of **9a** was light yellow in color, rather than red as with **8a**, and the observed $^{31}P\{^1H\}$ NMR spectrum revealed a single, well-resolved resonance at δ 58 (**9a**, Figure 5B) compared to δ 53 (**8a**). Interestingly, we noticed that by stirring **5** with an excess of $LiClO_4$ for a prolonged period of time (3 days, instead of 1 h), a new product formed, **10a**. Complex **10a** exhibits a sharp resonance at δ 38 in its in situ $^{31}P\{^1H\}$ NMR spectrum (Figure 5C). The solid-state identity of **10a** was confirmed by an X-ray crystallographic study of single crystals grown from the reaction mixture by layering Et_2O over a CH_2Cl_2 solution of this material. In the structure of **10a**, we observed a trans arrangement of ligands **4** around the Ni metal center (Figure 6B). Overall, these observations lead us to conclude that the formation of isomers **8a**, **9a**, and **10a** from **5** is a result of their energetic similarities. Compound **8a** can be viewed as a metastable intermediate between **9a** and **10a**. Complex **9a** is thermodynamically more stable than **10a**; indeed, **10a** will convert over time

Scheme 5. Reaction Scheme for the Formation of 9a and 9d, with Noncoordinating Counteranion Nickel(II) Salts[a]

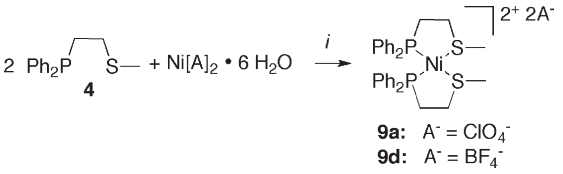

[a] (*i*) EtOH, 1 h.

to **9a**, but no significant conversion of **9a** to **10a** takes place under the conditions studied.

Because of our inability to characterize **8a** crystallographically, we decided to probe independent routes to these complexes via alternative syntheses. The addition of 2 equiv of ligand **4** dissolved in ethanol to an ethanol solution of nickel(II) perchlorate hexahydrate ($Ni[ClO_4]_2 \cdot 6H_2O$) (see **SAFETY NOTE**) resulted in the formation of a yellow powder that precipitated out of solution over the course of 1 h while the mixture was stirred vigorously (Scheme 5). After separation from the supernatant by filtration and drying, this powder was dissolved in CD_2Cl_2 and then characterized by $^{31}P\{^1H\}$ NMR spectroscopy, which showed a single sharp resonance at δ 58 (**9a**, Figure 5B). Notably, this $^{31}P\{^1H\}$ NMR resonance at δ 58 is distinct from that of **8a** isolated by chloride abstraction (δ 53) and identical to that seen from dissolving crystals grown from a solution of **8a** (δ 58). Single crystals grown by solvent layering of a CH_2Cl_2 solution of **9a** from this alternate synthesis (Scheme 5) with Et_2O were characterized by single-crystal X-ray diffraction analysis to reveal again the structure of **9a** (Figure 6A). Interestingly, when crystals from the same batch were dissolved in CH_2Cl_2, the observed $^{31}P\{^1H\}$ NMR resonance matched the resonance observed before crystallization (**9a**, δ 58). These observations confirm that the broad unresolved resonance seen at δ 53 (**8a**) when **5** is reacted with 2 equiv of $LiClO_4$ arises from a chemically identical, yet structurally unique species from **9a** and **10a** (Scheme 4).

Since the independent synthesis of square planar complex **9a** gave indirect proof of the existence of a different structural isomer with identical chemical composition, **8a**, we decided to characterize **5**, **8a**, **9a**, and **10a** using UV−vis spectroscopy. Each of these complexes has a different color (vide supra) and a distinct UV−vis signature. Crystallographically characterized square planar complexes **9a** and **10a** each exhibit a diagnostic d−d transition band at ~420 nm, while complex **8a** exhibits a red-shifted band at 499 nm with a substantially higher extinction coefficient (Figures SI-2, SI-3, and SI-4 and Table SI-1, Supporting Information), which can be an indicator of tetrahedral Ni(II) complexes.[55] Indeed, a higher extinction

dx.doi.org/10.1021/ja109624m | *J. Am. Chem. Soc.* 2011, 133, 3023–3033

coefficient is often indicative of the higher prevalence of antibonding and bonding orbital overlap between the ligands and d-orbitals of a Ni(II) center (P−Ni and S−Ni interactions) in a tetrahedral geometry.[56] In addition, this transition in **8a** (499 nm) is red-shifted from the square planar **9a** (424 nm) in solution, further evidence of the proposed tetrahedral structure (considering that d−d transitions become closer in energy in a tetrahedral species as compared to a square planar species).[55−60] Therefore, the proposed tetrahedral species **8a** can be viewed as an intermediate in the interconversion of **9a** and **10a** (Scheme 4). Note that we considered the potential for a weak interaction between the "non-coordinating" counterions within **8a** and the Ni center, but even at low temperature (203 K in CD_2Cl_2) with BF_4^- and PF_6^- as the counterions, we saw no evidence of such interaction by ^{11}B, ^{19}F, and ^{31}P NMR spectroscopies. This does not, however, completely discount the formation of five-coordinate intermediates with the counteranion.

We also decided to conduct further UV−vis experimentation on **7a′** in order to compare it to the other complexes (Scheme 3). We found that the extinction coefficient for **7a′** was higher than those of the octahedral complex **5** and square planar complexes **9a** and **9d** but lower than those of the proposed tetrahedral complexes **8a** and **8d** (Table SI-1, Supporting Information). In addition to this, the UV−vis spectrum shows more similarity to that of the *trans*-**10a**, than the proposed tetrahedral **8a** (Figure SI-2, Supporting Information), which is consistent with the trans arrangement of the 2 equiv of ligand **4** in the proposed structure of **7a′**. To further extend our understanding of this system, we proceeded to study other counterions in order to identify what conditions could control the formation of specific isomers during chloride abstraction.

All solution characterization of **10a** was limited to in situ techniques, where **10a** was generated from **5** by Cl^- ligand abstraction, since **10a** is less stable than both **8a** and **9a**. Indeed, if **10a** was prepared in CD_2Cl_2 and left in an NMR tube over a period of several weeks, the sharp single resonance observed by $^{31}P\{^1H\}$ NMR spectroscopy at δ 38 began to broaden with a gradual color change from yellow to red and growth of a new broad resonance at δ 54, assigned to **8a** (Scheme 2). This indicates that the stability of *trans*-**10a** is less than that of either proposed tetrahedral **8a** or cis-square planar **9a**.

Synthesis and Characterization of Cl^- Abstracted Complexes With Other "Noncoordinating" Counteranions: 8b−d, 9b,d, 10b,c. Proposed tetrahedral complex **8b** was generated by reacting octahedral complex **5** in CH_2Cl_2 with 2 equiv of sodium tetrakis-[3,5-bis(trifluoromethyl)phenyl]borate (NaBArF) followed by vigorous stirring for 1 h at room temperature (Scheme 2). The $^{31}P\{^1H\}$ NMR spectrum of this orange-red solution exhibits a single broad resonance at δ 60, consistent with quantitative formation of **8b**. Filtering this solution of **8b** to remove precipitated sodium chloride (NaCl), followed by solvent evaporation in vacuo, produced **10b** as a red-orange solid. This powder was redissolved in CH_2Cl_2 and layered with Et_2O in order to grow single crystals suitable for X-ray diffraction studies. The solid-state structure of **10b** like **10a** shows a trans arrangement of 2 equiv of ligand **4** around the Ni(II) center (Figure 6C). By comparing the structures of **10a** and **10b**, one can observe significant differences in bond angles and lengths around the metal center, which are likely the result of the difference in the steric bulk of the counterions and crystal packing (Table 1).[61−64] The Ni(II) centers in **10a** and **10b** adopt square planar geometries and share certain attributes. In particular, like **5**, the P1−Ni−S1 angle is smaller than the P1−Ni−S2 angle, due to the influence of the bite angle of ligand **4**.[51] This difference in observed angles

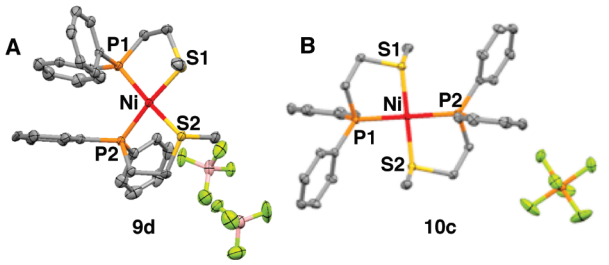

Figure 7. Single-crystal X-ray crystallographically derived structures of **9d** (A) and **10c** (B) with 50% thermal-ellipsoid probability. Hydrogen atoms are omitted for clarity; P = orange, S = yellow, Ni = red, C = gray, Cl = green, O = purple, F = light green, and B = light pink.

is exacerbated (Table 1) in the case of **10b**, which is likely a consequence of the larger BArF counteranion and corresponding crystal packing forces. While the Ni−P bond distances in the trans complexes **10a** and **10b** are slightly longer than the Ni−S bonds, the opposite is true in the cis complex **9a**, a consequence of the relative trans-donor abilities of the phosphine and thioether,[58] respectively.

When a CD_2Cl_2 solution of **5** was stirred with a slight excess of NaBArF, two resonances were observed by $^{31}P\{^1H\}$ NMR spectroscopy at δ 61 and 35 after only 1 h (Scheme 2). These are attributed to **9b** and **10b**, which are the cis and trans isomers, respectively. These assignments are consistent with our previous ones for **9a** and **10a**. The distribution of these isomers at room temperature is likely not representative of a thermodynamic equilibrium, since upon sequential cooling of these mixtures to 213 K the ratio of the isomers is not altered. Heating, unfortunately, results in decomposition.

The observation of the strong dependence of the geometry at the Ni(II) center on the counteranion in both solution and the solid-state prompted us to investigate this phenomenon further. Complexes **8c** and **10c** were prepared under conditions identical to those used to prepare **8a**, **9a**, and **10a**, but 2 equiv of thallium(I) hexafluorophosphate ($TlPF_6$) (**SAFETY NOTE**: Tl(I) salts are very toxic) were used as the abstracting agent in place of $LiClO_4$. In this case, a $^{31}P\{^1H\}$ NMR spectroscopic study revealed only one broad resonance at δ 53 (**8c**). Interestingly, the single crystals obtained using the same layering technique as previously described for **9a** and **10a**−**b** provided **10c**, which had a trans arrangement of the 2 equiv of ligand **4** around the metal center (Figure 7B). Dissolving these crystals of **10c** in CD_2Cl_2 and observing the resulting red solution by $^{31}P\{^1H\}$ NMR spectroscopy revealed a single broad resonance at δ 57, indicating that, in solution, the less stable trans product converts into the cis isomer **9c**, similar to the conversion of **10a** into **8a**.

As a final comparison in probing the effect of noncoordinating counteranion contributions on the geometry of this Ni(II) system, we investigated the syntheses of the square planar and proposed tetrahedral complexes using tetrafluoroborate (BF_4^-) salts (Scheme 2). Tetrahedral complex **8d** was prepared by adding 2 equiv of silver(I) tetrafluoroborate ($AgBF_4$) to a solution of **5** in CH_2Cl_2 and stirring vigorously for 1 h (Scheme 4). Removal of solvent in vacuo revealed a red powder, which exhibits a broad singlet at δ 55 in CD_2Cl_2 in its $^{31}P\{^1H\}$ NMR spectrum. This resonance is consistent with the formation of the tetrahedral complex (vide supra). Much like the structural change seen for **8a** converting to **9a** under solvent layering crystallization conditions, when a CH_2Cl_2 solution of **8d** was layered with Et_2O on top

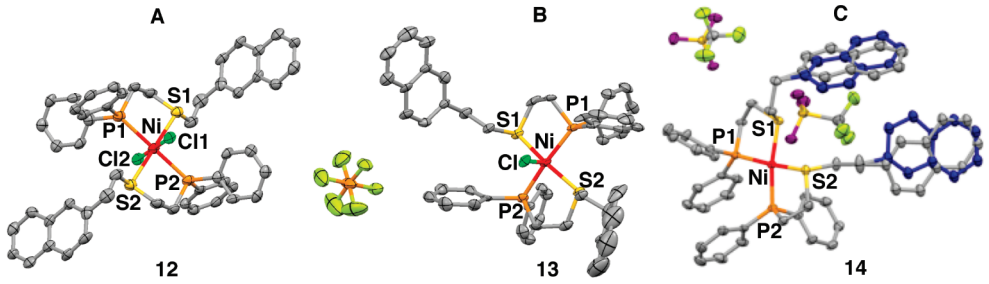

Figure 8. Single-crystal X-ray crystallographically derived structures of **12** (A), **13** (B), and **14** (C) with 50% thermal-ellipsoid probability. Hydrogen atoms are omitted for clarity; P = orange, S = yellow, Ni = red, C = gray, and Cl = green. Blue corresponds to a refined C disorder in the naphthalene group.

Scheme 6. Reaction Scheme for the Formation of 12−14, Where R = (2-Naphthalene)ethyl[a]

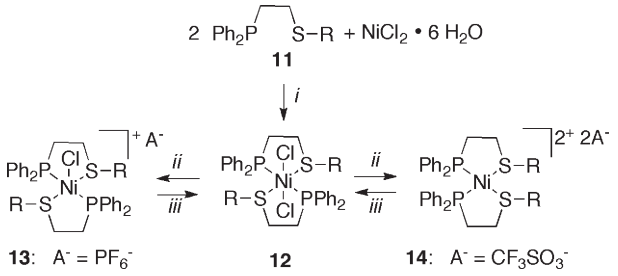

[a] (i) EtOH, 1 h; (ii) 2 equiv of $Tl(CF_3SO_3)$ (**14**) or 1 equiv of $TlPF_6$ (**13**) in CH_2Cl_2; (iii) 1 or 2 equiv of PPN^+Cl^- in CH_2Cl_2.

in an NMR tube, pale yellow crystals formed. An X-ray diffraction study conducted on these crystals revealed the structure of **9d**, which has a cis-square planar arrangement of 2 equiv of ligand **4** (Figure 7A). Similar to the crystal structure of the cis-square planar complex **9a**, **9d** exhibits shorter Ni−P bonds than Ni−S bonds, again in contrast to the observed trend for the trans complexes **10a−c**. The trend of the bite angle contributing to a smaller P1−Ni−S1 bond angle than the P1−Ni−P2 bond angle also holds. Finally, the bite angle in **9d** is nearly identical to the one in **9a**.

Complex **9d** also can be synthesized directly by reacting 2 equiv of ligand **4** with an ethanol solution of $Ni[BF_4]_2 \cdot 6H_2O$, a reaction analogous to the one used to prepare ClO_4^--containing complex **9a** from $Ni[ClO_4]_2 \cdot 6H_2O$. After the mixture containing 2 equiv of ligand **4** and 1 equiv of $Ni[BF_4]_2 \cdot 6H_2O$ was vigorously stirred for 1 h at room temperature (Scheme 5), a microcrystalline yellow powder precipitated and was recovered by filtration. $^{31}P\{^1H\}$ NMR spectroscopic analysis of this powder dissolved in CD_2Cl_2 showed a single resonance at δ 58, consistent with the formation of **9d**. An X-ray diffraction study of single crystals grown by layering Et_2O over a CH_2Cl_2 solution of this material confirmed the identity of this complex as **9d**. When these single crystals are dissolved in CD_2Cl_2 and characterized by $^{31}P\{^1H\}$ NMR spectroscopy, they show a singlet at δ 58, which is diagnostic of **9d**. Consistent with the results for single crystals of **9a** grown from a solution of **8a**, dissolving crystals of **9d** grown from a CH_2Cl_2 solution of **8d** and subsequent characterization by $^{31}P\{^1H\}$ NMR spectroscopy shows a single resonance at δ 58. A comparison of the UV−vis spectra for **8d** and **9d** respectively shows that proposed tetrahedral complex **8d** exhibits a band at 506 nm that has a significantly higher extinction coefficient than the analogous band at 420 nm for the square planar complex **9d** (Figures SI-3 and SI-4 and Table SI-1, Supporting Information). These data are analogous to what was observed for **8a** and **9a** and consistent with literature model complexes and spectroscopic assignments.[55]

The complexes formed with the various counterions exhibit qualitatively similar chemistry (but with different transformation rates between the three isomers **8**, **9**, and **10**; Scheme 2), in addition to some deviations in their $^{31}P\{^1H\}$ NMR spectra. Although we were unable to determine a specific reason for these observations, these counteranions have inherent differences in size and degree of electron delocalization. Others have previously observed how these properties affect reactivity in related coordination complexes.[61−64]

One important feature of all the Cl^--abstracted Ni(II) complexes in this study (**7a′**, **8a−d**, **9a−d**, **10a−c**) is that they can be quantitatively converted back to the starting material **5** by the addition of bis(triphenylphosphine)iminium chloride (PPN^+Cl^-) (Scheme 2). In addition to providing further evidence for the proposed structures, these reactions show how elemental anions such as Cl^- can be used to control the orientation of pendant groups in tweezer complexes. Such capabilities are important in the design of more sophisticated allosteric structures, and the cis to trans isomerization reactions common to this family of Ni complexes may become a powerful new pathway for controlling architecture that is not characteristic of the previously studied isolectronic WLA Rh(I), Pt(II), and Pd(II) systems.[1,20,21,25−28,30]

Synthesis and Characterization of Complexes 12, 13, and 14. In the interest of using these previous findings to probe the generality of the aforementioned reactions with respect to functionalized phosphinoalkyl thioether ligands, we synthesized a series of model complexes **12−14** (Scheme 6). Similar to the synthesis of **5**, by reacting 2 equiv of a (2-(2-naphthalene)-thioethyl)ethyldiphenylphosphine ligand, **11** (P,S-NAP; see Experimental Section), with $NiCl_2 \cdot 6H_2O$, we prepared and were able subsequently to isolate a new complex, **12** (Scheme 6). The solid-state structure of **12** was determined by a single-crystal X-ray diffraction study carried out with crystals grown by layering Et_2O on top of a CH_2Cl_2 solution of this material. In the solid state, complex **12** has an octahedral geometry similar to that observed for **5**, and its fluxional behavior as observed by $^{31}P\{^1H\}$ NMR spectroscopy shows remarkable similarities as well (Figures 8A and SI-5, Supporting Information). All other characterization data are consistent with the proposed structural formulation of **12**.

Interestingly, the mono-Cl^- adduct complex **13** can be synthesized from **12** by the addition of 1 equiv of $TlPF_6$ (see **SAFETY NOTE**) in CH_2Cl_2. This red compound, when dissolved in CD_2Cl_2, showed a single resonance in its $^{31}P\{^1H\}$ NMR spectrum at δ 51. Single crystals of **13** suitable for an X-ray diffraction study were grown by layering Et_2O on top of a CH_2Cl_2 solution of **13**.

dx.doi.org/10.1021/ja109624m | J. Am. Chem. Soc. 2011, 133, 3023–3033

Table 2. Selected Bond Length and Bond Angle Data for the Crystallographically-Derived Structures of 10b,c, 9d, and 12−14

bond lengths (Å)	10b	10c	9d	12	13	14
P1−Ni	2.2124(4)	2.2320(11)	2.1779(16)	2.509 (2)	2.203 (3)	2.1740(6)
P2−Ni	2.2124(4)	2.2320(11)	2.1710(16)	2.509 (2)	2.197 (3)	2.1777(7)
S1−Ni	2.1934(4)	2.1940(14)	2.2133(17)	2.454 (2	2.211 (3)	2.2155(7)
S2−Ni	2.1934(4)	2.1940(14)	2.2140(16)	2.454 (2)	2.234 (3)	2.2138(6)
Cl1−Ni	n/a	n/a	n/a	2.3635(17)	2.456 (3)	n/a
Cl2−Ni	n/a	n/a	n/a	2.3636(17)	n/a	n/a
bond angles (deg)	**10b**	**10c**	**9d**	**12**	**13**	**14**
P1−Ni−P2	180.0	180.0	98.24(6)	180.0	166.85(13)	99.43(2)
P1−Ni−S1	86.779(15)	87.22(5)	86.77(6)	84.38(8)	87.07(12)	86.31(2)
P1−Ni−S2	93.221(15)	92.78(5)	171.88(7)	95.62(8)	90.81(13)	170.15(3)
P2−Ni−S1	93.221(15)	92.78(5)	174.04(6)	95.62(8)	90.44(12)	170.69(3)
P2−Ni−S2	86.779(15)	87.22(5)	87.94(6)	84.38(8)	87.70(12)	86.97(2)
S1−Ni−S2	180.0	180.0	87.39(6)	180.0	162.51(12)	88.35(3)

A single-crystal X-ray diffraction study shows that **13** (Figure 8B) is a square-pyramidal complex with two fully chelated equivalents of phosphinoalkyl thioether ligand **11** around the Ni center in a trans arrangement with a single apical Cl^- ligand. Since **5** and **12** are isoelectronic and coordinatively isostructural, structure **13** provides further evidence of **7a′** (compare Schemes 3 and 6). The X-ray crystal structure of **13** exhibits a Ni−Cl bond longer [2.456(3) Å, Table 2] than the Ni−Cl bonds in **12** [2.3635(17) Å, Table 2]. This Ni−Cl bond length is the longest observed for all crystallographically characterized Ni(II) complexes discussed in this paper. Interestingly, in **13** the two Ni−S bond lengths are almost identical to the two Ni−P bond lengths.

It was also possible to isolate an analogue of **9a** and **9d** for complex **12** under complete chloride-abstracting conditions. The addition of 2 equiv of thallium(I) triflate [$Tl(CF_3SO_3)$] (see **SAFETY NOTE**) to a solution of **12** in CH_2Cl_2 yielded a deep red solution, which when filtered and reduced to dryness under vacuum gave a red powder, **14**. When this powder was dissolved in CD_2Cl_2 and characterized by $^{31}P\{^1H\}$ NMR spectroscopy, it showed a single resonance at δ 58. Layering Et_2O on top of a solution of **14** in CH_2Cl_2 yielded single crystals suitable for an X-ray diffraction study. This structural study showed a square-planar complex with a cis arrangement of 2 equiv of **11** around the Ni center, similar to that observed in the complexes with ligand **4** (**9a**, **9d**). The crystal structure of **14** exhibited Ni−P and Ni−S bond lengths, which were very similar to the isoelectronic analogues **9a** and **9d**. As mentioned above, the conformational flexibility of the ethyl spacer and asymmetric attachment of the naphthalene to the S moiety on ligand **11** allows for multiple orientations, which creates disorder in the solid-state. Indeed, two dominant conformations were resolved in the refined crystal structure of **14** (the secondary positions for the naphthalene groups are shown in blue in Figure 8C).

Sequential cooling of **12** in CD_2Cl_2 (room temperature to 203 K) and concomitant monitoring by $^{31}P\{^1H\}$ NMR spectroscopy showed evidence for the same behavior observed for **5** under identical conditions (Figure SI-5, Supporting Information). The initially broad singlet observed at room temperature (δ 31) for **12** begins to sharpen with decreasing temperature until 245 K, where a second resonance appears at δ 55, similar to the resonances observed for **5** at δ 57 and 30 at these temperatures. Recall that the latter resonance is assigned to octahedral complex **5** and the former resonance at δ 57 was assigned to the Cl^-- dissociated adduct **7a**. Similarly, the resonances at δ 55 and 31 observed when cooling **12** to 245 K are assigned to the analogous octahedral and square-pyramidal complexes **12** and **13**, respectively. When the system is cooled to 223 K, a third resonance appears and resolves at δ 52 and remains significantly broader than the other resonances at δ 55 and 31 down to 203 K. The broad resonance at δ 52 is likely due to slowly exchanging structural isomers (with the square pyramidal complex **13**, there at least four likely conformational arrangements).

Compared to **5**, the solid-state structure of complex **12** shows slightly longer Ni−P bonds [2.509(2) Å, Table 2] and slightly shorter Ni−Cl bonds [2.3635(17) Å, Table 2]. All of the bond angles in **12** follow the same trends observed in **5**, with the angles between the coordinating moieties of ligand **11** (P1−Ni−S1, P2−Ni−S2) being slightly smaller than the angles between the coordinating moieties of the separate ligands (P1−Ni−P2, S1−Ni−S2).

CONCLUSIONS

We have synthesized and studied a new system consisting of Ni(II) complexes formed from P,S-alkyl hemilabile ligands and Ni(II) salts wherein transformations of complex geometry can be induced by the introduction or abstraction of a coordinating halide. These processes originate from an octahedral Ni complex (**5**) in which the Cl^- ligands and thioether moieties possess a high degree of lability. Consequently, the solid-state structure of **5** represents an average of the many subspecies that exist in solution, which arise from several exchange pathways. Some of these subspecies can be obtained directly by the controlled abstraction of Cl^- ligands, which provides a basis for regulated geometric switching around the Ni(II) center. It is also clear that the counterions in each of these complexes can have a significant effect on the isomeric distribution and exchange pathways based on the differences observed between complex behavior in the solution and solid states. These transformations are fundamentally different from the series of reactions previously studied involving halide-induced switching in analogous systems using Rh(I), Pt(II), and Pd(II). It is evident from these experiments that the Ni(II) chemistry in this context is much richer and more complex than the previously studied WLA systems, with a variety of new geometries and interconversions available, where many can be

obtained in a controlled fashion. On the basis of our studies, a mechanism that explains these geometrical transformations is proposed, where it is likely that a four-coordinate P,S-alkyl Ni(II) complex undergoes an isomerization via a transient tetrahedral intermediate (with or without a weak interaction from the noncoordinating ion) between a cis- and trans-square planar arrangement. The presence of Ni complexes in distorted tetrahedral geometries in addition to ones with square planar geometries is not without precedence; indeed, the work of Miedaner et al.[51] showed that Ni(II) and Ni(I) complexes with phosphine chelates (nonhemilabile) exhibit distinct tetrahedral and square planar geometries. They argue that since the potential energy surface of the Ni(II) system is fairly soft, a balance between these steric and electronic forces can create a "compromise" and allow for the formation of multiple geometries, as observed here.

In many ways this complicated puzzle highlights the plasticity of the Ni(II) environment and the fact that, while the chemistry is rich, characterization and application of these reactions can be a daunting task. This study provides a glimpse at the key compounds and intermediates that should prove useful in understanding the necessary reaction pathways for application in functionalized WLA complexes. For these reasons, Ni(II) chemistry provides a significant challenge and also an opportunity for use in a nontraditional WLA chemistry. The set of reactions discovered may allow one to use halide ions (and possibly other coordinating molecules) to allosterically trigger the interaction between two functional groups appended to the chalcogen moieties via a cis−trans isomerization. Ultimately, future success in these endeavors will depend on an in-depth understanding of how to control these switching processes by reaction conditions and judicious ligand design.

EXPERIMENTAL SECTION

Materials and Methods. All chemicals were purchased from Sigma-Aldrich and Strem Chemicals and used without further purification, unless otherwise specifically mentioned. All solvents (CH_2Cl_2, $CH_3CH_2OCH_2CH_3$, CH_3CH_2OH) were purchased from Sigma-Aldrich as anhydrous grade and used as received. The Ni salts containing a noncoordinating anion ($Ni[BF_4]_2\cdot 6H_2O$ and $Ni[ClO_4]_2\cdot 6H_2O$) and respective thallium(I) salts [$TlPF_6$ and $Tl(CF_3SO_3)$] were purchased from Strem Chemicals and used without further purification. The P,S-Me ligand was prepared according to previously published methods.[25] 2-(2-Naphthalene)ethyl bromide was prepared from (2-(2-naphthalene)ethanol by bromination under nitrogen with excess PBr_3 in anhydrous CH_2Cl_2 overnight in 67% yield.[65] All NMR spectra were recorded on a Bruker Avance 400 MHz equipped with a broad-band probe and TopSpin software. UV−vis spectra were obtained on a Varian Cary 5000 UV−vis−NIR spectrophotometer. Flash chromatography was preformed using a Biotage HPFC SP4 Flash Purification System on silica. All manipulations with Ni(II) complexes were done at ambient conditions, and phosphine ligands were synthesized and stored under inert atmosphere of N_2 using Schlenk techniques or a glovebox (Vacuum Atmospheres, Nexus).

Bond energies and orbital structures for **5**, **6**, and **7a** were obtained from DFT calculations based on the geometry-optimized version of the crystallographically determined structure of **5**, which was edited for **6** and **7a** with the ADF 2009.01 GUI. Complexes **7b**−**d** were constructed in the ADF 2009.01 GUI before geometry optimization. The optimization used basis sets containing triple-ζ functions with one polarization function (TZP), the local density approximation of Becke[66] and Perdew[67] with the associated default exchange and correlation corrections, and the density functional methods available in the Amsterdam Density Functional (ADF2009.01) suite on a 16-core Parallel Quantum Solutions (PQS) computational cluster. Relativistic corrections used ZORA (zero-order relativistic approximation), and core electrons were unrestricted.

Single crystals suitable for X-ray diffraction studies were mounted using oil (Infineum V8512) on a glass fiber. All measurements were made on a Bruker APEX-II CCD with graphite-monochromated Mo Kα radiation (**5**, **9d**, **10a**−**c**, **14**) or with graphite-monochromated Cu Kα radiation (**9a**, **12**, **13**). The data were collected at a temperature of 100(2) K using an APEX2 V2.1−4 (Bruker, 2007) detector and processed using SAINTPLUS from Bruker. The data were corrected using their respective linear absorption coefficients, μ, before being corrected for Lorentz and polarization effects. The structures were solved by direct methods and expanded using Fourier techniques. Neutral atom scattering factors were taken from Cromer and Waber.[68] Anomalous dispersion effects were included in F_{calc};[69] the values for Df′ and Df″ were those of Creagh and McAuley.[70] The values for the mass attenuation coefficients are those of Creagh and Hubbell.[71] All calculations related to these corrections were performed using the Bruker SHELXTL3 crystallographic software package.

***trans*-[κ_2-$(Ph)_2PCH_2CH_2SCH_3]_2Ni(Cl)_2$ (5).** A flask equipped with a magnetic Teflon-coated stir bar was charged with 0.059 g of $NiCl_2\cdot 6H_2O$ (0.25 mmol) in 5 mL of absolute EtOH. To this green solution was added 0.130 g of **4** (0.5 mmol). The mixture turned deep red in color almost immediately and was stirred for 1 h before all volatiles were reduced in vacuo, leaving a crystalline green powder in 99% yield. ^{1}H NMR (CD_2Cl_2, 400 MHz): δ 12.12, 7.73−7.52 (br m, 20H, Ar*H*), δ 5.10 (br s, 8H, $-CH_2-$), δ 2.47 (br s, 6H, $-CH_3$). $^{13}C\{^1H\}$ NMR (CD_2Cl_2, 100 MHz): δ 159.1 (br), δ 140.3 (br), δ 132.7 (sh), δ 132.5 (sh), δ 132.2 (sh), δ 129.8 (sh), δ 35.2 (br), δ 21.0 (br), δ 9.9 (br). $^{31}P\{^1H\}$ NMR (CD_2Cl_2, 161 MHz): δ 31.8 (br s). ESIMS (*m*/*z*) for $[M - Cl]^+$: calcd 613.0619, found 613.0265. Anal. Calcd for $C_{30}H_{34}Cl_2NiP_2S_2$: C, 55.41; H, 5.27; Cl, 10.90. Found: C, 53.42; H, 5.16; Cl, 10.62.

[κ_2-$(Ph)_2PCH_2CH_2SCH_3]_2NiCl[ClO_4]$ (7a′). A flask equipped with a magnetic Teflon-coated stir bar was charged with 0.100 g of **5** (0.15 mmol) in 5 mL of CH_2Cl_2. To the formed light red solution was added slowly 0.033 g (0.30 mmol) of $LiClO_4$ dissolved in a minimal amount of absolute EtOH. After 1 h of vigorous stirring, the mixture turned deep red in color and was filtered to remove LiCl before the solvent was removed in vacuo to reveal a crystalline red powder (0.107 g, 98%). ^{1}H NMR (CD_2Cl_2, 400 MHz): δ 7.23−7.51 (br s, 20H, Ar*H*), δ 3.06 (br s, 8H, $-CH_2-$), δ 2.77 (br s, 6H, $-CH_2-$), δ 2.02 (br s, 3H, $-CH_3$). $^{13}C\{^1H\}$ NMR (CD_2Cl_2, 100 MHz): δ 133.9 (m), δ 132.6 (sh), δ 129.4 (sh), δ 127.4 (br), δ 34.0 (sh), δ 31.2 (sh), δ 21.6 (sh). $^{31}P\{^1H\}$ NMR (CD_2Cl_2, 161 MHz): δ 52 (br s). ESIMS (*m*/*z*) for $[M - Cl]^+$: calcd 613.0619, found 613.0613. Anal. Calcd for $C_{30}H_{34}Cl_2O_4NiP_2S_2$: C, 50.45; H, 4.80. Found: C, 50.34; H, 4.87.

[κ_2-$(Ph)_2PCH_2CH_2SCH_3]_2Ni[ClO_4]_2$ (8a, 9a, 10a). **8a**: A flask equipped with a magnetic Teflon-coated stir bar was charged with 0.144 g of **5** (0.25 mmol) in CH_2Cl_2. To this was added 0.053 g of $LiClO_4$ (0.5 mmol) dissolved in absolute EtOH and the reaction was stirred for 1 h before all volatiles were removed in vacuo to yield a red solid in 98% yield. ^{1}H NMR (CD_2Cl_2, 400 MHz): δ 7.96−7.10 (br m, 20H, Ar*H*), δ 5.50 (br s, 8H, $-CH_2-$), δ 3.24−1.21 (br s, 6H, $-CH_3$). $^{13}C\{^1H\}$ NMR (CD_2Cl_2, 100 MHz): δ 140.5 (br), δ 134.0.8 (m), δ 131.8 (sh), δ 130.8 (sh), δ 129.3 (sh), δ 128.7 (sh), δ 30.1 (br), δ 25.5 (br), δ 16.2 (br). $^{31}P\{^1H\}$ NMR (CD_2Cl_2, 161 MHz): δ 53 (br s). Anal. Calcd for **8a**, $C_{30}H_{34}Cl_2NiO_8P_2S_2$: C, 46.30; H, 4.40. Found: C, 45.75; H, 4.82.

9a: A flask equipped with a magnetic Teflon-coated stir bar was charged with 0.130 g of **4** (0.5 mmol) in CH_2Cl_2. To this was added 0.091 g of $Ni[ClO_4]_2\cdot 6H_2O$ (0.25 mmol) and the reaction was stirred for 1 h during which time a yellow microcrystalline solid precipitated from solution. This solid was removed from the supernatant by filtration and dried on a glass frit. ^{1}H NMR (CD_2Cl_2, 400 MHz): δ 7.55−7.43 (br m, 20H, Ar*H*), δ 3.25−2.68 (br m, 16H, $-CH_2-$, $-CH_3$). $^{13}C\{^1H\}$

NMR (CD_2Cl_2, 100 MHz): δ 133.9 (sh), δ 129.8 (sh), δ 123.5 (br), δ 35.8 (br), δ 33.0 (br), δ 24.2 (br). $^{31}P\{^1H\}$ NMR (CD_2Cl_2, 161 MHz): δ 57 (br s). Anal. Calcd for **9a**, $C_{30}H_{34}Cl_2NiO_8P_2S_2$: C, 46.30; H, 4.40. Found: C, 45.91; H, 4.13.

10a: A flask equipped with a magnetic Teflon-coated stir bar was charged with 0.050 g of **5a** (0.076 mmol) in CH_2Cl_2. To this was added 0.050 g of $LiClO_4$ (0.46 mmol) and the reaction was stirred for 3 days until yellow powder precipitated from solution. The supernatant solution was separated and characterized by NMR, and single crystals suitable for X-ray diffraction were grown from this solution enabling the confirmation of the structure of **10a**. ^1H NMR (CD_2Cl_2, 400 MHz): δ 7.73−7.51 (br m, 20 H, Ar*H*), δ 2.66 (br m, 8H, $-CH_2-$), δ 2.12 (br m, 8H, $-CH_2-$), δ 1.27 (br s, 6H, $-CH_3$). $^{13}C\{^1H\}$ NMR (CD_2Cl_2, 100 MHz): δ 206.5 (sh), δ 133.6 (sh), δ 132.8 (m), δ 131.0 (br), δ 129.5 (sh), δ 129.0 (sh), δ 30.6 (sh), δ 29.7 (sh). $^{31}P\{^1H\}$ NMR (CD_2Cl_2, 161 MHz): δ 39 (br s).

κ_2-(Ph)$_2$PCH$_2$CH$_2$SCH$_3$]$_2$Ni[BArF]$_2$ (8b). A flask equipped with a magnetic Teflon-coated stir bar was charged with 0.144 g of **5a** (0.25 mmol) in CH_2Cl_2. To this was added 0.428 g of NaBArF (0.5 mmol) and the reaction was stirred for 1 h before being reduced under vacuum to reveal a yellow solid. ^1H NMR (CD_2Cl_2, 400 MHz): δ 7.73−7.22 (br m, 44H, Ar*H*), δ 2.98−2.66 (br m, 8H, $-CH_2-$, $-CH_3$) δ 1.98 (br s, 6H, $-CH_3$). $^{31}P\{^1H\}$ NMR (CD_2Cl_2, 161 MHz): δ 60. Anal. Calcd for $C_{94}H_{58}B_2F_{48}NiP_2S_2 \cdot CH_2Cl_2$: C, 47.73; H, 2.53. Found: C, 47.58; H, 2.32.

[κ_2-(Ph)$_2$PCH$_2$CH$_2$SCH$_3$]$_2$Ni[PF$_6$]$_2$ (8c). A flask equipped with a magnetic Teflon-coated stir bar was charged with 0.144 g of **5a** (0.25 mmol) in CH_2Cl_2. To this was added 0.177 g of $Tl(PF_6)$ (0.5 mmol) and the reaction was stirred for 1 h before being reduced under vacuum to reveal a red solid. ^1H NMR (CD_2Cl_2, 400 MHz): δ 8.66, 7.71−7.51, δ 7.06 (br s, 20H, ArH), δ 6.29 (br s, 8H, $-CH_2$), δ 2.74−2.49 (br m, 6H, $-CH_3$). $^{31}P\{^1H\}$ NMR (CD_2Cl_2, 161 MHz): δ 51 (br, s, cis), δ 37.7 (br, s, trans). Anal. Calcd for $C_{30}H_{34}F_{12}NiP_4S_2$: C, 41.45; H, 3.94. Found: C, 41.26; H, 3.65.

[κ_2-(Ph)$_2$PCH$_2$CH$_2$SCH$_3$]$_2$Ni[BF$_4$]$_2$ (8d, 9d). 8d: A flask equipped with a magnetic Teflon-coated stir bar was charged with 0.144 g of **5** (0.25 mmol) in CH_2Cl_2. To this was added 0.097 g of $AgBF_4$ (0.5 mmol) and the reaction was stirred for 1 h before being reduced in vacuo, leaving a red solid. ^1H NMR (CD_2Cl_2, 400 MHz): δ 7.69−7.40 (br m, 20H, Ar*H*), δ 3.70−1.30 (br m, 14H, $-CH_2-$, $-CH_3$). $^{13}C\{^1H\}$ NMR (CD_2Cl_2, 100 MHz): δ 144.6 (br), δ 135.1 (m), δ 131.9 (sh), δ 130.8 (br), δ 129.3 (m), δ 130.8 (sh), δ 128.8 (sh), δ 20.2 (br), δ 13.57 (br). $^{31}P\{^1H\}$ NMR (CD_2Cl_2, 161 MHz): δ 54 (br s). Anal. Calcd for **8d** $C_{30}H_{34}B_2F_8NiP_2S_2$: C, 47.85; H, 4.55. Found: C, 48.03; H, 4.58.

9d: A flask equipped with a magnetic Teflon-coated stir bar was charged with 0.130 g of **4** (0.5 mmol) in CH_2Cl_2. To this was added 0.091 g of $Ni[ClO_4]_2 \cdot 6H_2O$ (0.25 mmol) and the reaction was stirred for 1 h during which time a yellow microcrystalline solid precipitated from solution. This solid was removed from the supernatant by filtration and dried on a glass frit. ^1H NMR (CD_2Cl_2, 400 MHz): δ 7.56−7.44 (br m, 20H, Ar*H*), δ 3.20 (br s, 4H, $-CH_2-$), δ 2.70−2.59 (br m, 10H, $-CH_2-$, $-CH_3$). $^{13}C\{^1H\}$ NMR (CD_2Cl_2, 100 MHz): δ 133.8 (sh), δ 133.3 (sh), δ 129.8 (sh), δ 123.4 (m), δ 35.3 (m), δ 32.8 (m), δ 23.9 (m). $^{31}P\{^1H\}$ NMR (CD_2Cl_2, 161 MHz): δ 58 (br, s). Anal. Calcd for **9d**, $C_{30}H_{34}B_2F_8NiP_2S_2$: C, 47.85; H, 4.55. Found: C, 47.60; H, 4.12.

(2-(2-Naphthalene)thioethyl)ethyldiphenylphosphine (11). 2-(2-Naphthalene)ethyl bromide was dissolved in acetonitrile (20 mL) and added to a solution 2-(diphenylphosphine)ethanethiol[72] (1 equiv) premixed with potassium *tert*-butoxide (1 equiv) in acetonitrile in a glovebox for 1 h at room temperature. This suspension was stirred overnight and then passed through a layer of Celite, and all volatile residues were removed in vacuo. The resulting oil was subjected to a chromatographic purification (Flash 40+M column, *n*-hexanes/dichloromethane 8% → 66%, 1320 mL, flow rate 40 mL/min), which afforded **11** as a clear, analytically pure oil (3.4 g, 43%). ^1H NMR (400 MHz, CD_2Cl_2, 22 °C): δ 7.78−7.31 (br, m, 15H, Ar*H*), δ 2.99−2.98 (br, m, 2H, $-CH_2-$), δ 2.89−2.87 (br, m, 2H, $-CH_2-$), δ 2.65−2.61 (br, m, 2H, $-CH_2-$), δ 2.38−2.35 (br, m, 2H, $-CH_2-$). $^{31}P\{^1H\}$ NMR (161 MHz, CD_2Cl_2, 22 °C): δ −17.0 (s).

***trans*-[κ_2-(Ph)$_2$PCH$_2$CH$_2$SCH$_2$CH$_2$-(2-naphthalene)]$_2$Ni(Cl)$_2$ (12).** A flask equipped with a magnetic Teflon-coated stir bar was charged with 0.500 g (2.1 mmol) of nickel(II) chloride hexahydrate ($NiCl_2 \cdot 6H_2O$) in ethanol at room temperature. To this mixture was added 2 equiv of ligand **11** (P,S-NAP) (1.686 g, 4.2 mmol) dissolved in a minimum amount of CH_2Cl_2. The resulting mixture was stirred for 1 h, causing the color of the solution to change from pale green to deep red. The solvent was removed in vacuo to yield a fine crystalline green powder (1.9 g, 97%). ^1H NMR (400 MHz, CD_2Cl_2, 22 °C): δ 7.78−7.73, δ 7.44 (br, s, Ar*H*, 34 H); δ 3.7−1.25 (br, s, $-CH_2-$, 16 H). $^{13}C\{^1H\}$ NMR (CD_2Cl_2, 100 MHz): δ 168.5 (br), 156.5 (br), 147.6 (br), 138.9 (br), 134.7 (sh), 134.2 (sh), 133.0 (sh), 132.8 (sh), 132.5 (sh), 131.6 (m), 130.5 (m), 130.0 (m), 129.6 (sh), δ 128.6 (sh), δ 128.3 (sh), δ 128.0 (sh), δ 127.8 (sh), δ 127.5 (sh), δ 126.8 (sh), δ 126.7 (sh), δ 126.2 (sh), δ 126.0 (sh), δ 41.3 (br), δ 39.1 (br), δ 36.7 (br), δ 32.9 (br), δ 23.2 (br). $^{31}P\{^1H\}$ NMR (161 MHz, CD_2Cl_2, 22 °C): δ 30.9 (br, s). ESIMS (*m*/*z*) $[M - Cl]^+$: calcd 893.1871, found 893.1895. Anal. Calcd for $C_{52}H_{50}Cl_2NiP_2S_2$: C, 67.11; H, 5.42. Found: C, 65.28; H, 5.22.

***trans*-[κ_2-(Ph)$_2$PCH$_2$CH$_2$SCH$_2$CH$_2$-(2-naphthalene)]$_2$NiCl[PF$_6$] (13).** One equivalent of thallium(I) hexafluorophosphate ($TlPF_6$) (0.038 g, 0.107 mmol) was added to a solution of **12** (0.100 g, 0.107 mmol) in CH_2Cl_2 and stirred for 1 h. The solution was filtered and solvent was removed in vacuo, yielding a crystalline red powder (0.103 g, 93%). ^1H NMR (400 MHz, CD_2Cl_2, 22 °C): δ 7.77, δ 7.75−7.08 (br, m, Ar*H*, 34 H); δ 2.95, δ 2.80, δ 2.63 (br, m, $-CH_2-$, 16 H). $^{31}P\{^1H\}$ NMR (161 MHz, CD_2Cl_2, 22 °C): δ51.4 (br, singlet). ESIMS (*m*/*z*) $[M - PF_6]^+$: calcd 893.1871, found 893.1859. Anal. Calcd for $C_{52}H_{50}ClF_6NiP_3S_2$: C, 60.05; H, 4.85. Found: C, 62.75; H, 4.93.

***cis*-[κ_2-(Ph)$_2$PCH$_2$CH$_2$SCH$_2$CH$_2$-(2-naphthalene)]$_2$Ni[CF$_3$SO$_3$]$_2$ (14).** A flask equipped with a magnetic Teflon-coated stir bar was charged with 2 equiv of thallium(I) triflate $[Tl(CF_3SO_3)]$ (0.76 g, 0.21 mmol), in a solution of **12** (0.100 g, 0.107 mmol) in CH_2Cl_2, and was allowed to stir for 1 h. The resulting mixture was filtered and the solvent removed in vacuo, leaving a red powder (0.214 g, 88%). ^1H NMR (400 MHz, CD_2Cl_2, 22 °C): δ 7.48−7.13 (br, m, Ar*H*, 34 H); δ 3.07−1.59 (br, m, $-CH_2-$, 16 H). $^{31}P\{^1H\}$ NMR (161 MHz, CD_2Cl_2, 22 °C): δ 57.5 (br, s). Anal. Calcd for $C_{54}H_{50}F_6NiO_6P_2S_4$: C, 56.02; H, 4.35. Found: C, 56.73; H, 4.27.

■ ASSOCIATED CONTENT

Supporting Information. Additional NMR data, UV−vis spectra, a table of extinction coefficients, computational data, details on X-ray experimental procedures, and CIF files. This material is available free of charge via the Internet at http://pubs.acs.org.

■ AUTHOR INFORMATION

Corresponding Author
chadnano@northwestern.edu

■ ACKNOWLEDGMENT

We thank Northwestern IMSERC for analytical instrumentation. M.R.J. acknowledges Northwestern University for a Ryan Fellowship and the NSF for a Graduate Research Fellowship. C.A.M. is grateful to NSF, ARO, and AFOSR-MURI for generous funding. The authors are grateful to Dr. Robert Kennedy for useful discussions regarding the manuscript.

REFERENCES

(1) Holliday, B. J.; Mirkin, C. A. *Angew. Chem., Int. Ed.* **2001,** *40,* 2022.
(2) Dietrich, B.; Guilhem, J.; Lehn, J.-M.; Pascard, C.; Sonveaux, E. *Helv. Chim. Acta* **1984,** *67,* 91.
(3) Dietrich-Buchecker, C. O.; Sauvage, J. P.; Kern, J. M. *J. Am. Chem. Soc.* **1984,** *106,* 3043.
(4) Jude, H.; Sinclair, D. J.; Das, N.; Sherburn, M. S.; Stang, P. J. *J. Org. Chem.* **2006,** *71,* 4155.
(5) Johnson, D. W.; Raymond, K. N. *Inorg. Chem.* **2001,** *40,* 5157.
(6) Knight, L. K.; Freixa, Z.; van Leeuwen, P. W. N. M.; Reek, J. N. H. *Organometallics* **2006,** *25,* 954.
(7) Liu, Y.; Flood, A. H.; Stoddart, J. F. *J. Am. Chem. Soc.* **2004,** *126,* 9150.
(8) McClure, B. A.; Rack, J. J. *Angew. Chem., Int. Ed.* **2009,** *48,* 8556.
(9) Swiegers, G. F.; Malefetse, T. J. *Chem. Rev.* **2000,** *100,* 3483.
(10) Carlucci, L.; Ciani, G.; Proserpio, D. M. *Coord. Chem. Rev.* **2003,** *246,* 247.
(11) Kay, E. R.; Leigh, D. A.; Zerbetto, F. *Angew. Chem., Int. Ed.* **2007,** *46,* 72.
(12) Farrell, J. R.; Mirkin, C. A.; Guzei, I. A.; Liable-Sands, L. M.; Rheingold, A. L. *Angew. Chem., Int. Ed.* **1998,** *37,* 465.
(13) Dixon, F. M.; Eisenberg, A. H.; Farrell, J. R.; Mirkin, C. A.; Liable-Sands, L. M.; Rheingold, A. L. *Inorg. Chem.* **2000,** *39,* 3432.
(14) Gianneschi, N. C.; Cho, S.-H.; Nguyen, S. T.; Mirkin, C. A. *Angew. Chem., Int. Ed.* **2004,** *43,* 5503.
(15) Liu, X.; Stern, C. L.; Mirkin, C. A. *Organometallics* **2002,** *21,* 1017.
(16) Gianneschi, N. C.; Mirkin, C. A.; Zakharov, L. N.; Rheingold, A. L. *Inorg. Chem.* **2002,** *41,* 5326.
(17) Eisenberg, A. H.; Ovchinnikov, M. V.; Mirkin, C. A. *J. Am. Chem. Soc.* **2003,** *125,* 2836.
(18) Jeon, Y.-M.; Heo, J.; Brown, A. M.; Mirkin, C. A. *Organometallics* **2006,** *25,* 2729.
(19) Slone, C. S.; Mirkin, C. A.; Yap, G. P. A.; Guzei, I. A.; Rheingold, A. L. *J. Am. Chem. Soc.* **1997,** *119,* 10743.
(20) Khoshbin, M. S.; Ovchinnikov, M. V.; Mirkin, C. A.; Zakharov, L. N.; Rheingold, A. L. *Inorg. Chem.* **2005,** *44,* 496.
(21) Wiester, M. J.; Ulmann, P. A.; Mirkin, C. A. *Angew. Chem., Int. Ed.* **2010,** *50* (1), 114–137.
(22) Kovbasyuk, L.; Kramer, R. *Chem. Rev.* **2004,** *104,* 3161.
(23) Takeuchi, M.; Ikeda, M.; Sugasaki, A.; Shinkai, S. *Acc. Chem. Res.* **2001,** *34,* 865.
(24) Eisenberg, A. H.; Dixon, F. M.; Mirkin, C. A.; Stern, C. L.; Incarvito, C. D.; Rheingold, A. L. *Organometallics* **2001,** *20,* 2052.
(25) Ulmann, P. A.; Brown, A. M.; Ovchinnikov, M. V.; Mirkin, C. A.; DiPasquale, A. G.; Rheingold, A. L. *Chem.-Eur. J.* **2007,** *13,* 4529.
(26) Masar, M. S.; Mirkin, C. A.; Stern, C. L.; Zakharov, L. N.; Rheingold, A. L. *Inorg. Chem.* **2004,** *43,* 4693.
(27) Brown, A. M.; Ovchinnikov, M. V.; Mirkin, C. A. *Angew. Chem.* **2005,** *117,* 4279.
(28) Yoon, H. J.; Mirkin, C. A. *J. Am. Chem. Soc.* **2008,** *130,* 11590.
(29) Yoon, H. J.; Kuwabara, J.; Kim, J.-H.; Mirkin, C. A. *Science* **2010,** *330,* 66.
(30) Gianneschi, N. C.; Nguyen, S. T.; Mirkin, C. A. *J. Am. Chem. Soc.* **2005,** *127,* 1644.
(31) Koga, T.; Furutachi, H.; Nakamura, T.; Fukita, N.; Ohba, M.; Takahashi, K.; Ōkawa, H. *Inorg. Chem.* **1998,** *37,* 989.
(32) Colpas, G. J.; Maroney, M. J.; Bagyinka, C.; Kumar, M.; Willis, W. S.; Suib, S. L.; Baidya, N.; Mascharak, P. K. *Inorg. Chem.* **1991,** *30,* 920.
(33) Li, Y.; Zamble, D. B. *Chem. Rev.* **2009,** *109,* 4617.
(34) Barondeau, D. P.; Kassmann, C. J.; Bruns, C. K.; Tainer, J. A.; Getzoff, E. D. *Biochemistry* **2004,** *43,* 8038.
(35) Trofimenko, S.; Calabrese, J. C.; Kochi, J. K.; Wolowiec, S.; Hulsbergen, F. B.; Reedijk, J. *Inorg. Chem.* **1992,** *31,* 3943.
(36) Baidya, N.; Olmstead, M.; Mascharak, P. K. *Inorg. Chem.* **1991,** *30,* 929.
(37) Holm, R. H.; Chakravorty, A.; Dudek, G. O. *J. Am. Chem. Soc.* **1963,** *85,* 821.
(38) Schumann, M.; Elias, H. *Inorg. Chem.* **1985,** *24,* 3187.
(39) Chakravorty, A.; Fennessey, J. P.; Holm, R. H. *Inorg. Chem.* **1965,** *4,* 26.
(40) James, T. L.; Smith, D. M.; Holm, R. H. *Inorg. Chem.* **1994,** *33,* 4869.
(41) Panda, R.; Zhang, Y.; McLauchlan, C. C.; Venkateswara Rao, P.; Tiago de Oliveira, F. A.; Münck, E.; Holm, R. H. *J. Am. Chem. Soc.* **2004,** *126,* 6448.
(42) James, T. L.; Cai, L.; Muetterties, M. C.; Holm, R. H. *Inorg. Chem.* **1996,** *35,* 4148.
(43) Rigo, P.; Bressan, M.; Basato, M. *Inorg. Chem.* **1979,** *18,* 860.
(44) Dilworth, J. R.; Wheatley, N. *Coord. Chem. Rev.* **2000,** *199,* 89.
(45) Kim, J. S.; Reibenspies, J. H.; Darensbourg, M. Y. *Inorg. Chim. Acta* **1996,** *250,* 283.
(46) Kim, J. S.; Reibenspies, J. H.; Darensbourg, M. Y. *J. Am. Chem. Soc.* **1996,** *118,* 4115.
(47) Ge, P.; Riordan, C. G.; Yap, G. P. A.; Rheingold, A. L. *Inorg. Chem.* **1996,** *35,* 5408.
(48) Jalil, M. A.; Fujinami, S.; Senda, H.; Nishikawa, H. *J. Chem. Soc., Dalton Trans.* **1999,** 1655.
(49) Green, M. L. H. *J. Organomet. Chem.* **1995,** *500,* 127.
(50) Mizuno, J. *J. Phys. Soc. Jpn.* **1961,** *16,* 1574.
(51) Miedaner, A.; Haltiwanger, R. C.; DuBois, D. L. *Inorg. Chem.* **1991,** *30,* 417.
(52) Wiester, M. J.; Braunschweig, A. B.; Mirkin, C. A. *Inorg. Chem.* **2010,** *49,* 7188.
(53) Meier, P. F.; Merbach, A. E.; Dartiguenave, M.; Dartiguenave, Y. *Inorg. Chem.* **1979,** *18,* 610.
(54) Basolo, F.; Johnson, R. C. *Coordination Chemistry: The Chemistry of Metal Complexes*; W. A. Benjamin, Inc.: New York, 1964.
(55) Nelson, S. M.; Shepherd, T. M. *J. Chem. Soc.* **1965,** 3276.
(56) Ebsworth, E. A. V.; Rankin, D. W. H.; Cradock, S. *Structural Methods in Inorganic Chemistry*; CRC Press: Boston, 1991.
(57) Hollas, J. M. *Modern Spectroscopy*; John Wiley & Sons, Ltd: Hoboken, NJ, 2004.
(58) Huheey, J. E.; Keiter, E. A.; Keiter, R. L. *Inorganic Chemistry: Principles of Structure and Reactivity*; Harper Collins College Publishers: New York, 1993.
(59) Collman, J. P., Hegedus, L. S., Norton, J. T., Finke, R. G. *Principles and Applications of Organotranstion Metal Chemistry*; University Science Books: Sausalito, CA, 1987.
(60) Miessler, G. L.; Tarr, D. A. *Inorg. Chem.*; 3rd ed.; Prentice Hall: Upper Saddle River, NJ, 2004.
(61) Strauss, S. H. *Chem. Rev.* **1993,** *93,* 927.
(62) Reed, C. A. *Acc. Chem. Res.* **1998,** *31,* 133.
(63) Krossing, I.; Raabe, I. *Angew. Chem., Int. Ed.* **2004,** *43,* 2066.
(64) Macchioni, A. *Chem. Rev.* **2005,** *105,* 2039.
(65) Kim, D. W.; Hong, D. J.; Seo, J. W.; Kim, H. S.; Kim, H. K.; Song, C. E.; Chi, D. Y. *J. Org. Chem.* **2004,** *69,* 3186.
(66) Becke, A. D. *Phys. Rev. A* **1988,** *38,* 3098.
(67) Perdew, J. P.; Yue, W. *Phys. Rev. B* **1986,** *33,* 8800.
(68) Cromer, D. T.; Waber, J. T. *International Tables for X-ray Crystallography*; The Kynoch Press: Birmingham, England, 1974; Vol. IV.
(69) Ibers, J. A.; Hamilton, W. C. *Acta Crystallogr.* **1964,** *17,* 781.
(70) Creagh, D. C.; McAuley, W. J. *International Tables for Crystallography*; Kluwer Academic Publishers: Boston, 1992; Vol. C.
(71) Creagh, D. C.; Hubbell, J. H. *International Tables for Crystallography*; Kluwer Academic Publishers: Boston, 1992; Vol. C.
(72) Chat, J.; Dilworth, J. R.; Schmultz, J. A.; Zubieta, J. A. *J. Chem. Soc., Dalton Trans.* **1979,** 1595.